Computers and Electrical Engineering 131 (2026) 110976

Contents lists available at ScienceDirect

Computers and Electrical Engineering

journal homepage: www.elsevier.com/locate/compeleceng

A game-theoretic approach to fair and grid-aware load flexibility allocation in residential distribution networks

Gabriel Gómez-Ruiz *, Jesús Clavijo-Camacho, Reyes Sánchez-Herrera, José M. Andújar

Research Centre CITES, University of Huelva, 21007 Huelva, Spain

ARTICLE INFO

Keywords:
Fairness
Game theory
Load flexibility
Phase unbalance
Power quality
Residential distribution network
Thermostatically controlled load

ABSTRACT

This article evaluates the potential of thermostatically controlled loads (TCL) as flexible resources to improve power quality–particularly phase unbalance–in low-voltage residential distribution networks while ensuring fair consumer participation. To address both grid-level and social objectives, the adaptive fairness and grid-aware allocation (AFGA) algorithm is proposed. This algorithm integrates cooperative game theory and Nash bargaining principles to jointly optimize phase balancing and consumer utility. The proposed approach dynamically allocates residential consumer flexibility by accounting for phase-level constraints, individual flexibility capacity, and historical participation, thereby preventing the persistent overuse of specific consumers and promoting equitable long-term engagement. Simulation results on a representative residential network with 100 households demonstrate that, with only 20% participation, the AFGA algorithm reduces the unbalance load factor (ULF) to below 10%, achieves a highly equitable distribution of benefits (Gini index = 0.065), and effectively enforces adaptive fairness through penalty-feedback mechanisms. Furthermore, the algorithm completes a full-day simulation in 102 s with only 0.24 MB of peak memory usage. These findings position the AFGA algorithm as an effective and scalable solution for integrating fairness-aware residential flexibility into the operation of low-voltage residential distribution networks.

1. Introduction

Phase unbalance is a common issue in low-voltage three-phase distribution networks due to uneven single-phase connections across phases. Studies in Europe and the US show that over half of distribution feeders experience significant unbalance, where one phase can carry over 50% more load than another. A phase unbalance scenario can lead to increased losses, equipment overheating, and premature equipment failure [1,2].

Phase unbalance causes current unbalance, which in turn is considered the primary source of voltage unbalance. According to international standards such as EN 50160 and IEC 61000-3 series, the voltage unbalance in low and medium voltage systems must remain below 2% when measured over 10-minute intervals [3]. In low-voltage residential networks, this 2% voltage unbalance limit typically corresponds to phase current unbalances in the range of 10-20% [4], although the exact ratio depends on the network configuration and load distribution.

* Corresponding author.
E-mail address: gabriel.gomez@diesia.uhu.es (G. Gómez-Ruiz).

https://doi.org/10.1016/j.compeleceng.2026.110976
Received 23 August 2025; Received in revised form 30 December 2025; Accepted 12 January 2026
Available online 15 January 2026

List of symbols

$\mathcal{N}$	set of residential consumers
$i \in \mathcal{N}$	index for consumer i
$t \in \mathcal{T}$	discrete time step in the planning horizon
$\mathcal{P} = \{A, B, C\}$	set of three electrical phases
$\phi \in \mathcal{P}$	electrical phase assigned to consumer i
$\mathcal{N}_\phi$	subset of consumers connected to phase ϕ
$d_{i,t}$	baseline (nominal) demand of consumer i at time t
$f_{i,t}$	flexibility potential of consumer i at time t
$x_{i,t}$	decision variable: adjustment to demand of consumer i at time t
$P_{i,t}(x_{i,t})$	adjusted real power of consumer i at time t
$Q_{i,t}(x_{i,t})$	reactive power of consumer i at time t
PF	power factor
V_{phase}	phase-to-neutral voltage magnitude
$I_{i,t}(x_{i,t})$	complex current magnitude of consumer i at time t
$I^{agg}_{\phi,t}$	aggregated current of all consumers on phase ϕ at time t
I^{max}_t	maximum phase current at time t
I^{avg}_t	average phase current at time t
$ULF_t(x)$	unbalance load factor at time t under allocation x
ULF^{base}_t	baseline unbalance load factor
ULF_{max}	maximum allowed unbalance load factor
$R_{i,t}$	reward for consumer i at time t
p_t	dynamic price signal at time t
$D_{i,t}$	discomfort cost for consumer i at time t
β_i	discomfort sensitivity parameter of consumer i
$U_{i,t}$	fairness penalty for consumer i at time t
$\alpha_{i,t}$	fairness sensitivity coefficient for consumer i at time t
$x^{fair}_{i,t}$	fair contribution of consumer i at time t
ε	constant for numerical stability
λ	adaptation rate for fairness penalty update
γ	smoothing coefficient for fair share updates
$\mathcal{J}_{cons}(x)$	total consumer utility objective function
$\mathcal{J}_{grid}(x)$	total grid-level utility objective function
$\mathcal{J}(x)$	combined optimization objective function
$\mathcal{C}_1$	grid reward coefficient for ULF reduction
$\mathcal{C}_2$	grid cost coefficient for procuring flexibility

Mitigating phase unbalance in low-voltage residential networks has become a priority [5,6], and a range of strategies has emerged. Traditional approaches include manual load re-phasing–reconnecting certain customers to different phases–and the use of phase balancers or balancing transformers. However, these methods are often labor-intensive and slow to respond to dynamic changes [1]. Recent research highlights demand-side flexibility as a dynamic tool for phase balancing. Flexible loads, such as thermostatically controlled loads (TCL) [7], can be coordinated to redistribute phase loading in real time. In particular, direct load control (DLC) programs enable grid operators or aggregators to temporarily adjust the operation of flexible appliances in exchange for incentives [8]. This allows for either a reduction in energy consumption during high-demand periods (peak shaving) or an increase during low-demand periods (valley filling) [9]. Consequently, integrating coordinated control of these appliances into residential demand response (RDR) programs allows utilities to manage grid constraints directly, effectively reducing phase load asymmetry and maintaining voltage unbalance within regulatory thresholds [10–13].

An RDR program that relies solely on TCL uses the inherent flexibility of common household appliances, such as dishwashers, electric water heaters, heat pumps, and refrigerators, to adjust or shift their power consumption. TCL are well-suited for RDR programs because their thermal inertia allows for short-term changes in electricity consumption with minimal impact on user comfort. These devices operate using thermostats and alternate between on and off states within a temperature deadband, effectively acting as distributed energy storage by modulating power around a baseline while maintaining temperature within acceptable limits. By slightly adjusting setpoints or duty cycles, aggregated TCL can deliver significant load reductions or increases on demand, helping balance the grid without noticeable effects on consumers [14]. A project conducted in Yukon, Canada, demonstrated that RDR can effectively reduce winter peak electricity demand, achieving up to 0.65 kW demand savings per home with a 3°C setback. Preheating strategies ensured minimal comfort impact, with 82% of participants reporting no noticeable temperature changes and none opting out due to

discomfort [15].

As RDR programs evolve, there is growing emphasis on fairness, especially as more users interact directly with energy systems. The benefits shared between consumers–and the burdens associated with flexibility allocation–must be distributed equitably among participants. To address this, game-theoretical techniques are increasingly employed to ensure fair outcomes. In cooperative game formulations applied to low-voltage residential networks, a Nash bargaining solution can determine the demand reductions assigned to each user, aligning with grid objectives while adhering to a specific fairness principle, such as equity or meritocracy [16].

1.1. Literature review

While recent literature has made significant advances in various aspects of RDR programs, including infrastructure, control, policy, security, and scalability, a critical gap remains in addressing both grid-level objectives, such as mitigating phase unbalance, and fairness in utility distribution and flexibility allocation. Studies such as [11,17,18] focus on improving grid performance, particularly in unbalanced three-phase networks, by adjusting the phase-sequence of households using flexibility provided solely by TCL [17], or by combining flexibility from TCL and photovoltaic systems [11,18]. However, these approaches do not address fairness and therefore overlook the interaction between social equity among consumers and grid-level objectives.

Related efforts in home energy management (HEM) and demand response aggregation–such as the combined integer programming and reinforcement learning (RL) framework for battery energy storage system (BESS) management proposed in [19], and the three-level optimization of active distribution systems incorporating competition among aggregators introduced in [20]–illustrate the increasing sophistication of coordination and optimization mechanisms. However, these approaches do not explicitly address phase-level fairness. Similarly, advanced operational models for distribution networks, such as the phase shifting-soft open point (PS-SOP) proposed in [21], enhance system flexibility and efficiency through specialized hardware solutions but do not incorporate equity considerations. In parallel, decentralized system architectures–where decision-making, control, and coordination are distributed among multiple independent agents–have gained increasing attention, particularly in the form of peer-to-peer (P2P) energy trading and networked microgrids. Game-theoretic methods have been widely applied in this context, for example to optimize the sizing of networked microgrids [22] or to incentivize user participation in P2P energy trading [23].

At the same time, recent advances in the literature increasingly recognize the importance of fairness in energy systems. However, most existing fairness-aware demand response schemes focus primarily on economic dimensions, such as incentive distribution, user prioritization, or billing mechanisms, with limited consideration of physical grid constraints. For example, studies [24] and [25] introduce fairness through game-theoretic approaches and Shapley value-based billing schemes, ensuring equitable benefit allocation among participating users. While effective from an economic and strategic perspective, these approaches do not explicitly address distribution network characteristics and operational challenges, such as phase-level load imbalance or power quality constraints.

In contrast, the algorithm proposed in this article explicitly incorporates phase-level constraints while ensuring fairness through an adaptive control strategy grounded in cooperative game theory. The algorithm is evaluated using a representative low-voltage residential distribution network with 100 households, in which phase connections and appliance-level flexibility are explicitly modeled. This testbed is intentionally selected to isolate and analyze the mechanisms that generate phase unbalance at the residential level–namely, the random assignment of households to phases and the heterogeneous flexibility of TCL–while allowing a focused evaluation of equitable phase balancing among participating users. Although widely used benchmark feeders such as the IEEE 123-bus system [11,20,21], which provide detailed medium-voltage unbalanced network models and are well-suited for feeder-level validation, their use is not aligned with the objectives of this study.

1.2. Main contributions

This article introduces the adaptive fairness and grid-aware allocation (AFGA) procedure, designed to mitigate phase unbalance in residential low-voltage distribution networks through an adaptive and fairness-aware demand response mechanism. The AFGA procedure utilizes flexibility from residential users participating in a RDR program, aiming to balance loads across the phases. Unlike conventional models, where consumers enter predefined agreements to offer fixed controllable loads, the AFGA procedure is applied to a more complex, in terms of the optimization algorithm, and realistic scenario. In this approach, flexibility is modeled as a dynamic profile that evolves throughout the day, shaped by user behavior, usage patterns, and the specific appliance configurations of each household. This modeling approach allows grid operators to align demand adjustments with periods of sufficient user-side flexibility, enhancing both system performance and user acceptance. Fairness is ensured through a dynamically adaptive control mechanism

Table 1
Comparison of key features addressed by existing references in the literature and by the proposed AFGA procedure. An "X" indicates that a feature is addressed in the corresponding reference, while an '–' denotes its absence.

Reference	Economic incentives	Comfort	Historical participation	Phase balancing	Fairness mechanism
[11]	–	X	–	X	–
[17]	–	–	–	X	–
[24]	X	X	X	–	X
[25]	X	–	–	X	–
This work	X	X	X	X	X

grounded in cooperative game theory, specifically the Nash bargaining model. A fairness penalty is applied when individual contributions exceed their fair share, discouraging persistent overuse of flexibility from specific consumers. This time-aware fairness model ensures equitable utility distribution and encourages balanced participation across successive demand response events. The features of the AFGA procedure, particularly its integrated approach to phase balancing, fairness, and user-side dynamics, are summarized and compared with existing works in Table 1.

The rest of this article is organized as follows: Section 2 describes the materials and methods used. Section 3 introduces the proposed AFGA procedure. Section 4 presents the results of applying AFGA in key areas, including phase unbalance mitigation, benefit sharing, fairness enforcement, and computational performance. The article concludes with Section 5, which discusses the implications of the findings, and Section 6, which provides a summary of the conclusions.

2. Materials and methods

The materials and methods presented in this article describe the simulation environment, assumptions, and performance metrics used to develop and evaluate the proposed allocation procedure. The section begins by outlining the structure and characteristics of a representative low-voltage residential distribution network, including demand modeling and the quantification of phase unbalance. Next, it introduces an RDR program involving TCL and defines the flexibility profiles for participating households. Finally, it outlines the evaluation criteria used to assess both the technical performance and social fairness of the proposed algorithm.

2.1. Residential network model, demand profiles, and phase unbalance quantification

To explore demand-side flexibility in real-world distribution networks, a representative low-voltage residential scenario is considered, consisting of 100 residential consumers, each connected to a three-phase distribution feeder. This configuration replicates the architecture of many existing urban and suburban grids, where distribution networks must serve numerous small-scale consumers with unbalanced and variable demands [11,26].

In Fig. 1, each house (H_1 to H_n)–where n is the total number of houses–represents an individual residential consumer, modeled as a node in the distribution feeder. These consumers are randomly connected to the feeder phases (ϕ_A, ϕ_B, and ϕ_C) to emulate the uncoordinated phase allocation commonly found in existing residential distribution networks. This randomness introduces intrinsic phase-level unbalance, which, if left unmitigated, can degrade grid performance and increase operational costs. The houses are organized into energy communities, where an aggregator serves as the intermediary between the distribution system operator/balance responsible party (DSO/BRP) and the energy communities (EC). The aggregator receives flexibility requests from the DSO/BRP (either for load reduction or increase) and sends corresponding control signals to multiple home energy management system (HEMS) units. Each HEMS controls a set of TCL, including shiftable loads, whose operation can be rescheduled within predefined time windows, and curtailed loads, whose power consumption can be adjusted in real time to provide flexibility to the grid [27].

To reflect realistic daily consumption, each node is assigned a distinct stochastic demand profile generated using a time-of-day-

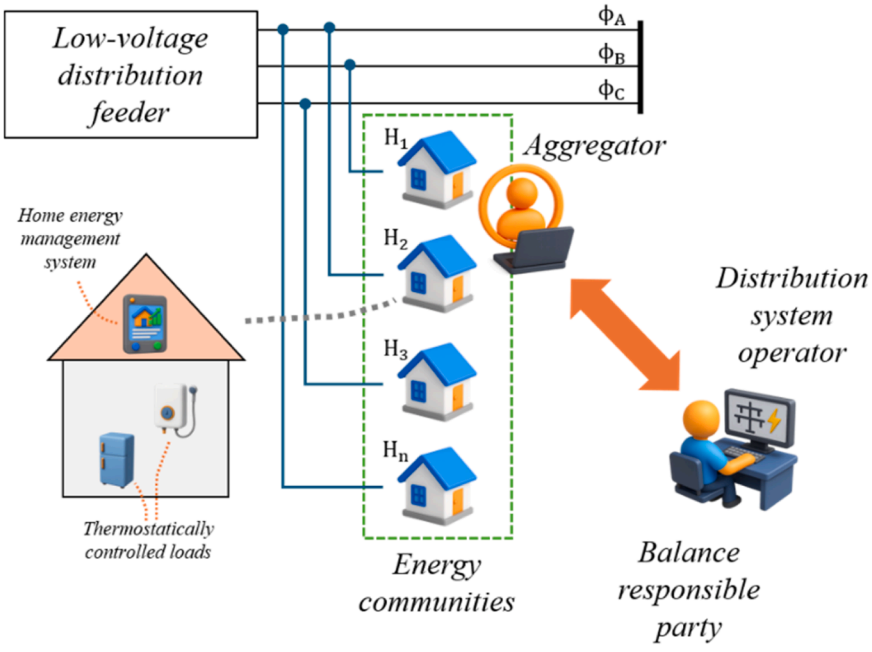

Fig. 1. Overview of the residential low-voltage distribution network scenario.

based approach. This approach simulates typical household behavior by structuring the day into four representative periods: nighttime (10 PM–6 AM), morning peak (6 AM–10 AM), daytime (10 AM–6 PM), and evening peak (6 PM–10 PM). Each period is associated with a characteristic demand range, modeled using uniform probability distributions to capture variability in typical usage: low consumption at night (0.1–0.8 kW), moderate daytime demand (0.3–2.0 kW), and higher peaks in the morning (1.8–4.0 kW) and evening (2.0–4.5 kW). To enhance realism, consumer-level heterogeneity is introduced by adding Gaussian noise (mean 0, standard deviation 0.15 kW) and applying individual multiplicative variations (±15%) to the base demand signal. This creates distinct profiles that reflect both common behavioral patterns and unique household-specific deviations. Demand values are constrained within a residentially plausible range (0.1–4.5 kW). Only demand is considered, with no incorporation of distributed generation (e.g., rooftop photovoltaic systems). This simplification is both intentional and realistic: although distributed energy resources are growing in prevalence, most households still lack photovoltaic systems or batteries, particularly in moderate and low-income neighborhoods. The parameters used for stochastic residential demand profile generation are summarized in Table 2.

The aggregate demand by phase reveals a clear unbalance throughout the day, which is measured using the unbalanced load factor (ULF) [11]. The ULF quantifies the percentage deviation of the phase with the highest load from the average phase load. It serves as a grid metric and is incorporated into both the objective function and constraints of the optimization procedure introduced in Section 3. Fig. 2 illustrates the aggregated demand profiles for each phase over a 24-hour horizon, highlighting the time-varying differences in load distribution among the three phases. The shaded gray area represents the instantaneous phase unbalance at each time step, providing a direct visualization of phase-level stress in the distribution feeder. These phase-level demand profiles are obtained by aggregating the demand of 100 residential consumers, each randomly assigned to one of the three phases, as described in this section.

Fig. 3 complements the previous figure by presenting the time series of the baseline ULF, overlaid with a red dashed line indicating a 10% current unbalance limit. This threshold is adopted in this article as the maximum allowable unbalance level, in accordance with the standards and considerations discussed above [3,4]. The baseline ULF is computed directly from the aggregated phase demand profiles shown in Fig. 2. As observed in Fig. 3, the ULF exceeds 10% at multiple time steps, indicating that the existing phase unbalance in the network violates acceptable operational limits during certain periods of the day. This observation motivates the need for corrective control actions, which are introduced in Section 2.2.

2.2. Demand response participation and appliance-level flexibility modeling

An RDR program, in which 20 out of 100 residential consumers voluntarily participate, is proposed to mitigate the unbalanced scenario identified in Section 2.1. This proportion—20%—represents a realistic starting point for a RDR program deployment, reflecting the limited initial willingness of residential users to engage in the initiative. Participating consumers contribute their residential load flexibility as a resource to the grid.

The available flexibility originates entirely from household appliances, specifically modeled as TCL [9,11]. As noted in Section 2.1, this approach does not consider any contribution from distributed generation. TCL are categorized into two types according to their flexibility characteristics. The first category includes shiftable loads, whose operation can be deferred within predefined time windows without compromising user comfort. The second comprises curtailed loads, whose consumption can be modulated while maintaining service and thermal comfort requirements. This modulation allows for decreasing energy consumption during peak periods or increasing it during off-peak periods, in accordance with implemented DLC programs [8]. The flexibility profile for each participating consumer is derived from their original demand profile using a rule-based algorithm that incorporates appliance types, power ratings and time-of-use patterns as described in [28]. This algorithm assumes appliance-level flexibility ratios: approximately 25% of the daily load is treated as shiftable, based on the nominal power demand of appliances such as dishwashers (10%) and electric water heaters (15%). These shiftable loads are activated exclusively during three predefined daily periods reflecting typical residential usage patterns: morning (6 AM–9 AM), midday (12 AM–2 PM), and evening (7 PM–10 PM). In parallel, 28% of the total load is assumed to be curtailable, based on the estimated contributions of refrigerators (8%) and heat pumps (20%), and is allowed to vary across the entire 24-hour period. To introduce consumer diversity and behavioral realism, both the shiftable and curtailed ratios are adjusted individually for each participating consumer using a uniformly distributed random multiplier within ±5% of the nominal values. A random subset of 20 consumers (20% of the population) is selected to participate, reflecting plausible initial engagement levels in a voluntary RDR program. For these participants, the algorithm produces flexibility profiles by applying the variable appliance-level ratios directly to their original demand profiles. Non-participating consumers are assumed to provide no flexibility, reinforcing

Table 2
Summary of stochastic residential demand profile generation parameters.

Period	Time interval	Probability distribution for power usage (kW)	Gaussian noise for consumer-level heterogeneity (kW)	Individual multiplicative variations	Plausible demand range (kW)
Nighttime	10 PM–6 AM	$P \sim u(0.1,\ 0.8)$	$\epsilon \sim \mathcal{N}(0,\ 0.15^2)$	±15%	0.1–4.5
Morning peak	6 AM–10 AM	$P \sim u(1.8,\ 4.0)$			
Daytime	10 AM–6 PM	$P \sim u(0.3,\ 2.0)$			
Evening peak	6 PM–10 PM	$P \sim u(2.0,\ 4.5)$			

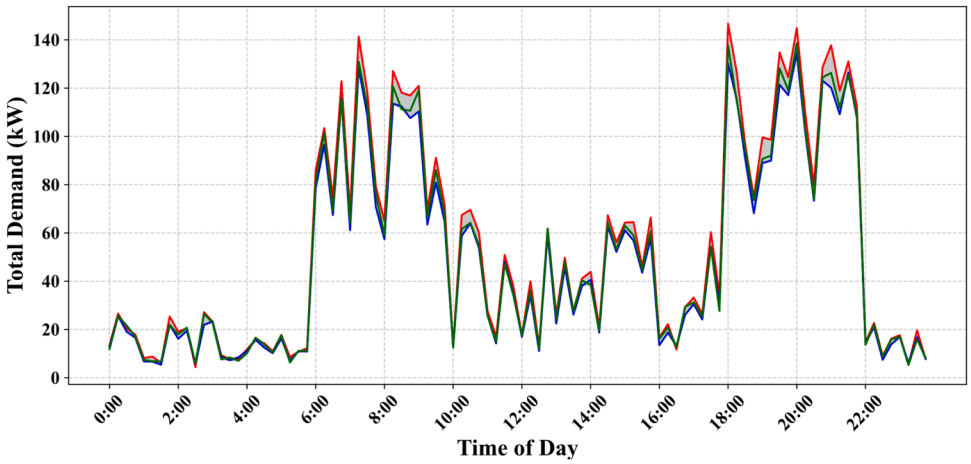

Fig. 2. Total demand profiles for each phase–phase A (red), phase B (blue), and phase C (green)–over a 24-hour period. The shaded gray area represents the unbalance between phases.

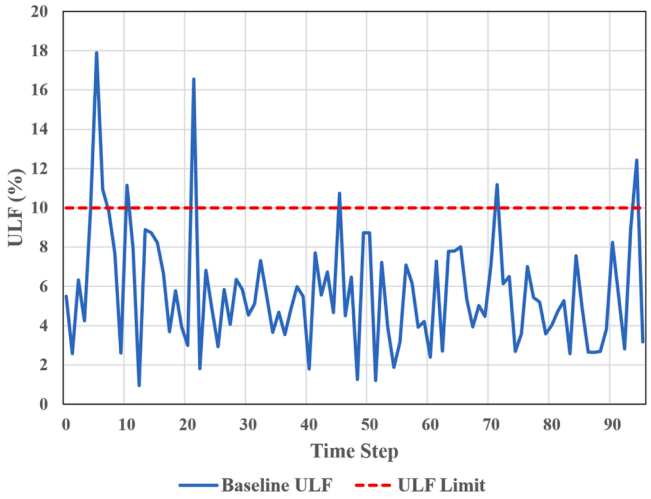

Fig. 3. Evolution of the baseline ULF (blue) across all time steps. The red dashed line indicates the operational threshold of 10%.

asymmetry in the grid and underscoring the need for optimization. Consequently, they do not receive direct economic benefits. This assumption is consistent with common practice in RDR programs [8]. The flexibility estimation process is inherently stochastic and serves to facilitate the preliminary application of the proposed allocation procedure. Its outputs provide a first-order approximation for evaluation under current assumptions, with the potential for refinement using real consumption data and more detailed appliance modeling in future work. A summary of the main parameters used to generate the flexibility profiles for each participating consumer is presented in Table 3.

Fig. 4 and Fig. 5 illustrate the decomposition of demand flexibility for two representative residential consumers—C14 (consumer 14) and C55 (consumer 55). In each figure, the solid blue line represents the original demand profile, the dashed orange line corresponds to the shiftable load component, and the dotted green line denotes the curtailed load component. The total flexibility available

Table 3
Parameters used for generation flexibility profiles, including participant selection, appliance-level flexibility ratios, and consumer diversity adjustments.

Category	Details
Participants	20 consumers (20% of total) participate. Non-participants provide no flexibility.
Appliance-level flexibility ratios	Shiftable loads: 25% of daily load, active only during three daily periods (6 AM–9 AM, 12 PM–2 PM, 7 PM–10 PM). Curtailed loads: 28% of daily load, adjustable at any time over the 24-hour period.
Consumer diversity	Individual ratios for shiftable and curtailed loads are adjusted using a uniformly distributed random multiplier within ±5% of the nominal values.

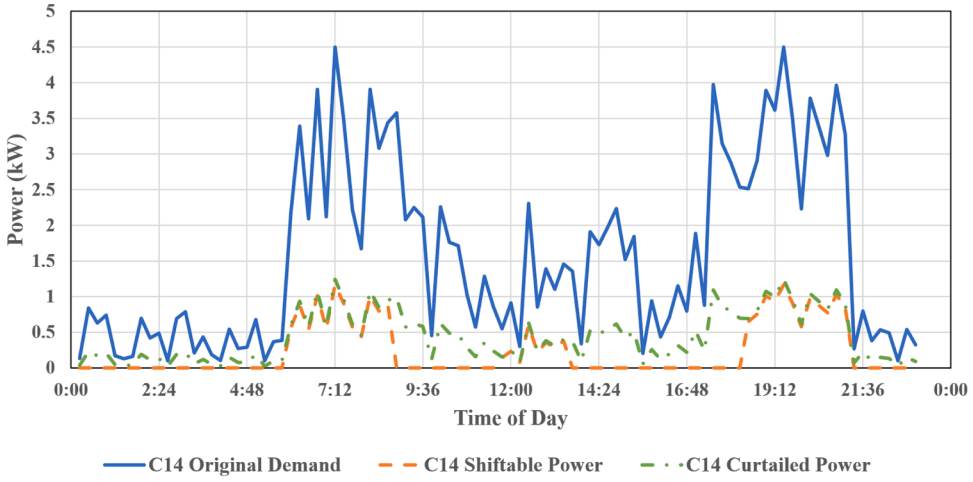

Fig. 4. Time series of consumer C14's original power demand (solid blue), shiftable power (dashed orange), and curtailed power (dotted green) over a 24-hour period.

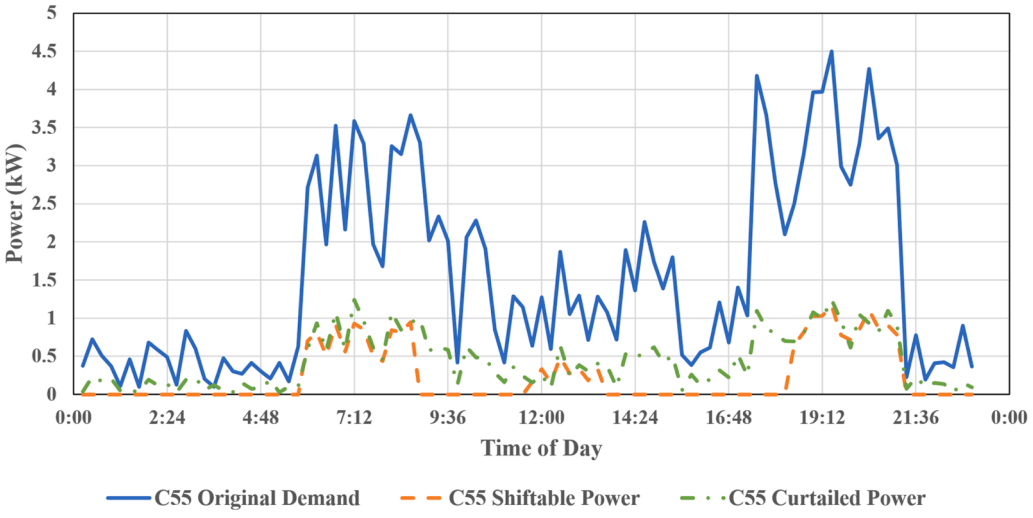

Fig. 5. Time series of consumer C55's original power demand (solid blue), shiftable power (dashed orange), and curtailed power (dotted green) over a 24-hour period.

to the algorithm at each time step is given by the combined contribution of the shiftable and curtailed components. These figures highlight how different types of flexible loads contribute to the overall adjustment potential at the individual consumer level.

2.3. Performance evaluation metrics

To evaluate the performance of the proposed allocation procedure, three key metrics are employed: the ULF, the Gini index, and the Pearson correlation coefficient. It is important to note that the fairness metrics reported in this article apply exclusively to participating consumers, reflecting the voluntary nature of the proposed RDR program.

The ULF serves as the primary metric for quantifying phase-level unbalance in the distribution feeder. It measures the percentage deviation of the phase with the highest current magnitude from the average across all three phases at each time step. The ULF is calculated dynamically throughout the simulation and plays a central role in the optimization model, appearing in both the objective function and the constraint set. A baseline ULF, computed from the original demand profiles prior to any RDR event, serves as a reference point for assessing improvement. In addition, an operational threshold of 10% is imposed in this article. The objective at each time step is to maintain the ULF below this threshold; once this condition is satisfied, reductions below the baseline ULF may be pursued if they yield economic benefits for the grid.

To assess fairness in the distribution of utility among participating consumers, the Gini index is applied [29]. This scalar metric quantifies inequality in the accumulated utility across all participants. A Gini value of 0 indicates perfect equality, while values closer

to 1 suggest disparity.

The Pearson correlation coefficient [30] is used to evaluate the effectiveness of the adaptive fairness control mechanism within the allocation procedure. Specifically, it measures the correlation between each consumer's deviation from their expected fair contribution and the corresponding penalty weight applied. A strong positive correlation indicates that the algorithm responds appropriately to repeated over-contribution by increasing the associated penalty, thereby discouraging sustained unfair participation.

Together, these three metrics provide a rigorous, multidimensional evaluation of the effectiveness of the allocation procedure, capturing both technical and social dimensions. The ULF reflects grid-level performance, the Gini index measures fairness in benefit distribution, and the Pearson coefficient assesses the responsiveness of the adaptive control mechanism.

Finally, the total computation time and peak memory usage required to optimize the load schedules across all participants over the entire planning horizon are calculated to assess the feasibility of the implementation in a real-world scenario.

To summarize the overall simulation framework and the interaction among its components, a schematic overview of the proposed system is presented in Fig. 6. The diagram illustrates the flow of information and control between the low-voltage residential distribution network–comprising participating households randomly connected to one phase of the distribution feeder–the residential appliances controlled by the AFGA algorithm based on consumer demand and flexibility profiles, and the performance evaluation layer, which assesses the effectiveness of the proposed approach in terms of phase load balancing across the distribution network and the utility allocated among participating consumers.

3. The adaptive fairness and grid-aware allocation procedure

3.1. Mathematical formulation of the AFGA model

3.1.1. Power and current modeling

To optimize residential flexibility in a three-phase distribution grid, it is essential to model how power consumption adjustments from individual consumers influence the electrical currents flowing through the feeder. This process begins with a representation of the power consumption behavior of each consumer and culminates in a phase-wise aggregation of complex currents, which is later used to evaluate grid unbalance.

A set of residential consumers denoted by $\mathcal{N}$ is considered, where each element $i \in \mathcal{N}$ indexes a unique consumer. Time is modeled as a sequence of discrete intervals $t \in \mathcal{T}$, representing uniform time slots over a planning horizon–specifically, 15-minute intervals throughout the day. Each consumer is associated with one of the three electrical phases, represented by the set $\mathcal{P} = \{A, B, C\}$, and let $\phi \in \mathcal{P}$ indicate the specific phase to which consumer i is connected. The subset of consumers on phase ϕ is denoted as $\mathcal{N}_\phi \subseteq \mathcal{N}$.

At each time t, the baseline power consumption of consumer i is given by the parameter $d_{i,t}$, which reflects the nominal demand before any RDR event. The decision variable in the optimization is $x_{i,t}$, which represents the adjustment applied to the baseline demand as a result of RDR events. This adjustment is restricted to the consumer's flexibility range, defined by $f_{i,t}$, which indicates the permissible deviation from the baseline. Note that a positive $x_{i,t}$ denotes increased consumption, while a negative value implies load

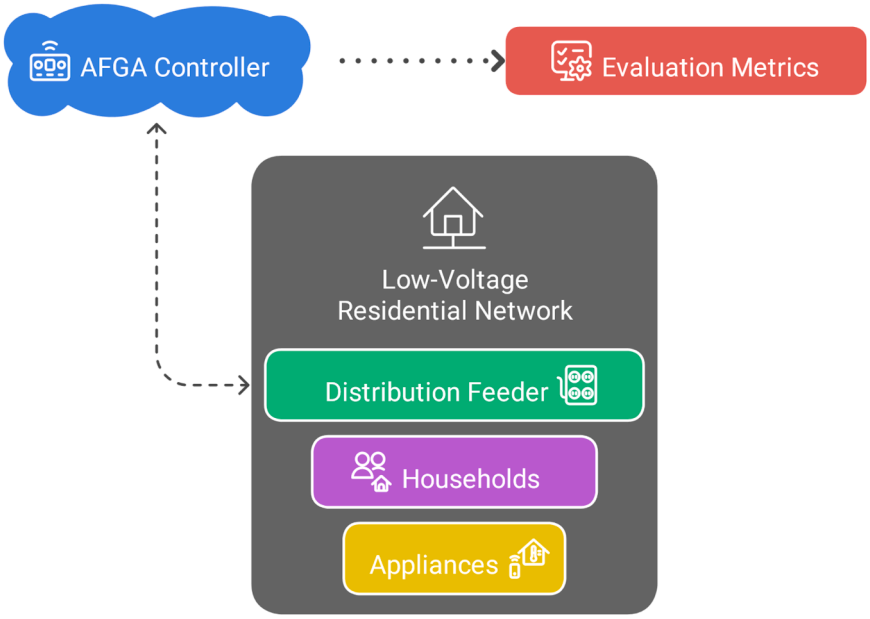

Fig. 6. Schematic representation of the simulation framework. The AFGA controller interacts with a low-voltage residential network composed of a distribution feeder, households, and flexible appliances. Performance is assessed using evaluation metrics that reflect both grid-level efficiency and consumer-level fairness.

reduction.

The adjusted real power consumption of consumer i at time t, incorporating RDR events, is given in Eq. (1):

$$P_{i,t}(x_{i,t}) = d_{i,t} + x_{i,t} \tag{1}$$

Eq. (1) directly models the net real power drawn from the grid after optimization adjustments. To fully capture the impact on the distribution feeder, the reactive power component must also be calculated. Assuming a constant power factor (PF), which is a grid parameter specified by the operator and maintained uniformly across consumers, the reactive power is derived using the trigonometric relation presented in Eq. (2):

$$Q_{i,t}(x_{i,t}) = P_{i,t}(x_{i,t}) \cdot \tan\left(\cos^{-1}(\mathrm{PF})\right) \tag{2}$$

The real and reactive power components are then used to compute the magnitude of the complex electrical current drawn by consumer i at time t. The calculation assumes a single-phase connection with a phase-to-neutral voltage magnitude V_{phase}. Using the apparent power relation for a single-phase system, the current magnitude is computed as given in Eq. (3):

$$I_{i,t}(x_{i,t}) = \frac{\sqrt{P_{i,t}(x_{i,t})^2 + Q_{i,t}(x_{i,t})^2}}{V_{phase}} \tag{3}$$

It is important to note that the load is considered inductive because the reactive power $Q_{i,t}$ is positive in this formulation, which corresponds to a lagging power factor–a typical characteristic of residential loads.

To evaluate grid-level impacts, the individual consumer currents are aggregated by phase. Specifically, for each phase $\phi \in \mathscr{P}$, the aggregated phase current magnitude flowing at time t is obtained by summing the current magnitudes of all consumers connected to that phase, as given in Eq. (4):

$$I^{agg}_{\phi,t} = \sum_{i \in \mathscr{N}_\phi} I_{i,t}(x_{i,t}) \tag{4}$$

Since the objective metric, i.e., the ULF, depends exclusively on current magnitudes, phase angles are not explicitly modeled in this formulation. This aggregated per-phase current will serve as the foundation for calculating the ULF, a metric that quantifies phase unbalance and is directly targeted in the optimization objective and constraints.

3.1.2. Unbalanced load factor

Eq. (4) gives the net complex-valued current resulting from the combined effect of all participating consumers on phase ϕ after demand response adjustments. To evaluate unbalance, the magnitudes of the phase currents are computed, and the maximum phase current is identified, as given in Eq. (5):

$$I^{max}_t = \max_{\phi \in \mathscr{P}} |I^{agg}_{\phi,t}| \tag{5}$$

Concurrently, the average magnitude of the phase currents is also computed to serve as a baseline for assessing deviation, as given in Eq. (6):

$$I^{avg}_t = \frac{1}{|\mathscr{P}|} \sum_{\phi \in \mathscr{P}} |I^{agg}_{\phi,t}| \tag{6}$$

where $|\mathscr{P}|$ is the cardinality of the phase set, which equals 3 in a standard three-phase system.

With the values provided by Eq. (5) and Eq. (6), the ULF at time t is computed as the percentage deviation of the most loaded phase from the average, as given in Eq. (7):

$$\mathrm{ULF}_t(x) = \frac{I^{max}_t - I^{avg}_t}{I^{avg}_t} \times 100 \tag{7}$$

In the context of the optimization model, the ULF is a dynamic, time-dependent function that depends on the decision variables $x_{i,t}$. Each adjustment in consumer load influences the aggregated currents $I^{agg}_{\phi,t}$, which in turn affect the ULF. This dependence allows the optimization to proactively manage phase balancing by adjusting demand in a coordinated manner across households. To establish a performance benchmark, the baseline ULF (ULF^{base}_t) is introduced. It is computed from the original consumption profile $d_{i,t}$, prior to any RDR event. This benchmark enables the model to quantify and reward improvements in phase balancing.

3.1.3. Objective function and constraints

The goal of the optimization model is to jointly maximize consumer satisfaction and grid performance while enforcing electrical and operational constraints. To this end, the objective function is carefully constructed to represent both sides of the system–consumer utility and grid-level rewards–while all decisions $x_{i,t}$ remain bounded within feasible flexibility limits and ensure compliance with system balancing requirements.

3.1.3.1. Consumer utility modeling. Each consumer $i \in \mathscr{N}$, at each time step $t \in \mathscr{T}$, is incentivized to participate in the RDR program by

adjusting their consumption, represented by decision variable $x_{i,t}$. The goal is to offer a net utility that fairly balances monetary reward, discomfort, and fairness considerations. The reward for participating is modeled as proportional to the absolute value of the flexibility adjustment, scaled by the dynamic price p_t, which varies with time and reflects market signals or system load, as given in Eq. (8):

$$R_{i,t} = p_t \cdot |x_{i,t}| \tag{8}$$

It is important to note that the reward formulation in Eq. (8) compensates consumers based on the magnitude of their flexibility provision rather than the direction of the adjustment. This modeling choice reflects flexibility-oriented demand response programs in which deviations from a baseline—either load reduction or load increase—are valuable to the grid [9]. In the simulation, the price signal p_t is stochastically generated to emulate realistic and time-varying incentives. Specifically, each value of p_t is sampled from a uniform distribution over the interval [0.1, 0.5] €/kWh, and then clipped with a minimum threshold of 0.2 €/kWh to avoid excessively low incentives.

However, modifying energy consumption often incurs discomfort, especially when the user is asked to change their regular consumption behavior. This is penalized quadratically using a consumer-specific discomfort parameter β_i, as given in Eq. (9):

$$D_{i,t} = \beta_i \cdot x_{i,t}^2 \tag{9}$$

A quadratic form is chosen because it reflects the fact that small deviations from normal behavior cause relatively little discomfort, while larger deviations cause disproportionately greater discomfort. This mirrors human response, where moderate changes are tolerable but extreme changes quickly become unacceptable. In the simulation, the parameter β_i is randomly assigned to each consumer to reflect heterogeneous sensitivity to consumption changes. Specifically, each β_i is independently drawn from a uniform distribution over the interval [0.01, 0.05].

In addition to accounting for user discomfort, the optimization introduces a fairness-aware penalty to address potential inequities in flexibility allocation. Each consumer i is expected to contribute a fair amount of flexibility, denoted $x_{i,t}^{\text{fair}}$, which is derived based on their relative capability within their assigned phase. The model penalizes only those deviations in which a consumer contributes more than their fair share. This asymmetry is intentional: it reflects the underlying principle that over-contribution, rather than under-participation, is the primary driver of long-term dissatisfaction and erosion of equity. The penalty is implemented using a smooth function scaled by a fairness sensitivity coefficient $\alpha_{i,t}$, which governs the strength of the penalty applied for unfair deviations. The penalty term is formulated in Eq. (10):

$$U_{i,t} = \alpha_{i,t} \cdot \log\left(\cosh\left(x_{i,t} - x_{i,t}^{\text{fair}}\right) + \varepsilon\right) \tag{10}$$

where ε is a small positive constant introduced to ensure numerical stability and to avoid taking the logarithm of zero. The choice of the $\log(\cosh(\cdot))$ function—commonly referred to as the log-cosh loss—is derived from [31]. It is smooth and differentiable, ensuring stable gradients, behaves quadratically for small deviations, and grows only linearly for large deviations. This balance of robustness, sensitivity to moderate errors, and mathematical smoothness makes it well-suited for fairness-aware optimization.

Combining all components, the net utility for consumer i at time t is computed as given in Eq. (11):

$$U_{i,t}^{\text{cons}} = \log\left(\max\left(R_{i,t} - D_{i,t} - U_{i,t}, \varepsilon\right)\right) \tag{11}$$

where the net utility is lower-bounded by ε to ensure that the logarithm remains well defined during numerical optimization. As a result, non-positive net utility values are treated as strongly penalized allocations.

This formulation is directly inspired by the Nash bargaining solution in cooperative game theory. In Nash's model, optimal allocations among agents are found by maximizing the product of utilities, subject to feasibility and individual rationality constraints. Taking the logarithm of each agent's utility function transforms the product into a sum of logarithms, which is computationally convenient and still reflects the same bargaining structure. This transformation also implicitly captures diminishing marginal returns, emphasizing proportional fairness over absolute gains.

By summing over all time steps and all participating consumers, the model arrives at the total consumer utility objective, as given in Eq. (12):

$$\mathscr{J}_{\text{cons}}(x) = \sum_{t \in \mathscr{T}} \sum_{i \in \mathscr{N}} U_{i,t}^{\text{cons}} \tag{12}$$

3.1.3.2. Grid-level objective. On the grid operator's side, the model integrates two performance indicators: reduction in ULF and the cost of procuring flexibility from consumers. At each time step t, the grid receives a reward proportional to the reduction in phase unbalance compared to the baseline. This is modeled using a grid reward coefficient $\mathscr{C}_1$, as given in Eq. (13):

$$G_t^{\text{reward}} = \mathscr{C}_1 \cdot \left(\text{ULF}_t^{\text{base}} - \text{ULF}_t(x)\right) \tag{13}$$

This term incentivizes reductions in ULF and aligns optimization with operational stability goals. At the same time, the cost to the grid for purchasing the flexibility from consumers is computed as the total amount of energy shifted (in absolute terms) multiplied by the current price of electricity and scaled by a cost coefficient $\mathscr{C}_2$, as given in Eq. (14):

$$G_t^{cost} = \mathscr{C}_2 \sum_{i \in \mathscr{N}} p_t \cdot |x_{i,t}| \tag{14}$$

The net grid-level objective across all time step is formulated in Eq. (15):

$$\mathscr{I}_{grid}(x) = \sum_{t \in \mathscr{T}} \left(G_t^{reward} - G_t^{cost}\right) \tag{15}$$

3.1.3.3. Combined optimization problem. To balance the interests of both stakeholders, the model combines the consumer and grid objectives into a single function, as given in Eq. (16):

$$\max_x \mathscr{I}(x) = \mathscr{I}_{cons}(x) + \mathscr{I}_{grid}(x) \tag{16}$$

For implementation in standard solvers such as sequential least squares programming (SLSQP), the maximization is equivalently written as a minimization of the negative objective, as given in Eq. (17):

$$\min_x -\mathscr{I}(x) \tag{17}$$

3.1.3.4. Constraints. To ensure the system operates within technical and fair bounds, several constraints are introduced. First, the ULF at each time must remain within a specified upper limit ULF_{max}, imposed by the grid operator to guarantee system safety, as given in Eq. (18):

$$ULF_t(x) \leq ULF_{max}, \ \forall t \in \mathscr{T} \tag{18}$$

In addition, the model enforces a minimum improvement threshold ε over the baseline, as given in Eq. (19):

$$ULF_t^{base} - ULF_t(x) \geq \varepsilon, \ \forall t \in \mathscr{T} \tag{19}$$

Lastly, the flexibility adjustments for each consumer must lie within the feasible range defined by their flexibility potential, as given in Eq. (20):

$$x_{i,t} \in \left[-f_{i,t}, f_{i,t}\right], \ \forall i \in \mathscr{N}, t \in \mathscr{T} \tag{20}$$

3.1.4. Fairness and penalty updates

The optimization model dynamically updates two components during its iterations: (1) the expected fair allocation of flexibility for each consumer, and (2) the fairness sensitivity penalty, which discourages deviation from this expected contribution. These mechanisms operate separately for each phase, utilizing the grouping of consumers into subsets $\mathscr{N}_\phi$ based on their assigned electrical phase $\phi \in \mathscr{P}$. Fairness is enforced within each phase to maintain symmetry and consistency in load balancing across the grid.

At each time step $t \in \mathscr{T}$, the expected fair contribution of each consumer $i \in \mathscr{N}_\phi$ is calculated by normalizing their flexibility potential $f_{i,t}$ relative to the total available flexibility on their phase. This ensures that consumers with higher capacity to adjust are expected to contribute more, but proportionally, according to Eq. (21):

$$x_{i,t}^{fair,new} = \frac{f_{i,t}}{\sum_{j \in \mathscr{N}_\phi} f_{j,t}} \cdot \sum_{j \in \mathscr{N}_\phi} |x_{j,t}| \tag{21}$$

This expression takes the total amount of phase-level flexibility actually used (i.e., the sum of $|x_{j,t}|$) and allocates it proportionally to each consumer based on their flexibility availability. The resulting $x_{i,t}^{fair,new}$ is an updated target that defines what would be a "fair" contribution for consumer i at time t.

However, because consumers may not be able to immediately align with newly calculated expectations, and to prevent abrupt or unstable shifts, the model applies a smoothing mechanism. This is done using an exponential moving average, controlled by a smoothing coefficient $\gamma \in [0, 1)$, which adjusts the sensitivity of updates, as given in Eq. (22):

$$x_{i,t}^{fair} \leftarrow \gamma x_{i,t}^{fair} + (1-\gamma) x_{i,t}^{fair,new} \tag{22}$$

In the simulation, the fair allocation matrix $x^{fair} \in \mathbb{R}^{N \times T}$ is initialized to zeros. At the first time step ($t = 0$), the initial fair contribution for each participating consumer is set phase-wise based on the mean flexibility within their phase. This bootstrapping ensures phase-level symmetry at the outset. For $t > 0$, the updated fair share is computed using the proportional allocation in Eq. (21) and then smoothed using the update rule in Eq. (22) with a fixed coefficient $\gamma = 0.5$.

The fairness-aware penalty, introduced in Eq. (10), is applied asymmetrically: it activates only when a consumer contributes more than their fair share. The strength of the penalty is modulated by $\alpha_{i,t}$, a sensitivity parameter that evolves over time to reflect observed deviations. Its update rule is given in Eq. (23):

$$\alpha_{i,t+1} \leftarrow \alpha_{i,t} \cdot \left(1 + \lambda \left| x_{i,t} - x_{i,t}^{fair} \right| \right) \tag{23}$$

Here, $\lambda > 0$ controls the rate of adaptation. This feedback loop allows the model to become increasingly responsive to repeated

over-contribution, reinforcing the protective mechanism for those consistently exceeding expectations. In the simulation, the initial values of $\alpha_{i,t}$ are generated independently for each consumer and time step by sampling from a uniform distribution between 0.01 and 0.1. This range provides diverse starting sensitivities across the population. Over time, $\alpha_{i,t}$ is updated dynamically according to the change in deviation between actual and fair flexibility allocations, with scaling controlled by the global parameter $\lambda = 0.2$ and normalized against the fair share to avoid instability near zero.

3.2. The proposed AFGA algorithm

This section presents the AFGA algorithm, a dynamic optimization procedure designed to coordinate RDR events across a multi-phase low-voltage distribution network. AFGA balances two key objectives: (1) maximizing consumer utility by incentivizing flexible energy consumption in a fair and discomfort-aware manner, and (2) improving grid stability by reducing phase unbalance, measured via the ULF. At each time step, the algorithm solves a constrained nonlinear optimization problem that jointly considers consumer-specific flexibility bounds, real-time price signals, phase-level fairness expectations, and grid-level performance metrics. The algorithm incorporates feedback mechanisms to adapt both the fair allocation targets and the sensitivity of fairness penalties over time. The complete step-by-step process is detailed in Algorithm 1.

Table 4 presents the simulation parameters and constants used in the implementation of the AFGA algorithm.

Although Table 4 presents a single set of parameters, these can be grouped into two categories. The algorithm coefficients $(\varepsilon, \lambda, \gamma)$ are generic control variables that influence numerical stability and convergence smoothness, and their selection does not alter the underlying optimization logic. The remaining values $(\mathrm{PF}, \mathrm{ULF}_{\max}, \mathrm{V}_{\mathrm{phase}}, \mathscr{C}_1, \mathscr{C}_2)$ reflect system-specific conditions or operator-defined thresholds. Their role is to ground the simulation in realistic grid operating conditions (e.g., voltage levels, permissible unbalance limits, cost coefficients), but they do not constrain the AFGA algorithm itself, which can be applied under alternative grid standards or system settings. More importantly, the testbed itself is stochastic: consumer demand profiles, phase allocations, flexibility ratios, and participant selection are all randomized within plausible ranges. Even though a single random seed is used for reproducibility, this modeling approach already embeds statistical diversity, making the reported outcomes representative of a wide range of plausible operating conditions.

4. Results

4.1. Comparative analysis of ULF before and after optimization

This subsection presents the evolution of the ULF before and after the application of the AFGA procedure. The objective is to assess the model's capacity to mitigate phase unbalance in the distribution grid by actively reshaping demand. Fig. 7 illustrates a time-series comparison between the baseline ULF, computed from the original consumption profile $\overline{P_{i,t}}$, and the adjusted ULF obtained after optimization-based load reshaping through the decision variable $x_{i,t}$, as defined in Eq. (1). The operational threshold for unbalance, set at 10%, is also indicated with a dashed red line for reference. Over the entire simulation horizon, the adjusted ULF consistently remains below the baseline ULF, demonstrating the effectiveness of the proposed AFGA model in mitigating phase unbalance through coordinated load control.

4.2. Grid and consumer benefit sharing

This subsection reports the economic outcomes of the optimization process, focusing on how the total benefits generated by the

Algorithm 1
Adaptive fairness and grid-aware allocation.

Input: Set of consumers $\mathscr{N}$, time steps $\mathscr{T}$, baseline demand $d_{i,t}$, flexibility bounds $f_{i,t}$, price signal p_t, discomfort coefficients β_i, fairness penalty weights $\alpha_{i,t}$, fairness allocation $x_{i,t}^{\mathrm{fair}}$, phase mapping $\phi(i)$, grid parameters (PF, $\mathrm{V}_{\mathrm{phase}}$, $\mathrm{ULF}_{\max}$, ε), grid-utility weighting factor $\mathscr{W}_{\mathrm{grid}}$
Output: Flexibility allocation $x_{i,t}$, adjusted unbalanced load factor $\mathrm{ULF}_t(x)$, updated fair share $x_{i,t}^{\mathrm{fair}}$, updated fairness penalties $\alpha_{i,t}$, fairness penalty values $U_{i,t}$

Initialize $x_{i,t} \leftarrow 0$, $\mathrm{ULF}_t^{\mathrm{base}}$, $\alpha_{i,t}$, and $x_{i,t}^{\mathrm{fair}}$
for t = 0 to $\mathscr{T} - 1$ **do**
  Extract $d_{i,t}$, $f_{i,t}$, p_t, β_i, $\alpha_{i,t}$, $x_{i,t}^{\mathrm{fair}}$
  Compute baseline $\mathrm{ULF}_t^{\mathrm{base}}$ using $d_{i,t}$
  Define the optimization problem based on the given objective and constraints
  Solve using SLSQP; store and clip result in $x_{i,t}$
  Update adjusted demand $P_{i,t}$ and compute $\mathrm{ULF}_t(x)$
  Compute new fair allocation $x_{i,t}^{\mathrm{fair.new}}$ over phase ϕ
  Smooth fair update $x_{i,t}^{\mathrm{fair}}$
  Update penalty weight $\alpha_{i,t+1}$
  Compute fairness penalties $U_{i,t}$
end **for**
return $x_{i,t}$, $\mathrm{ULF}_t(x)$, $x_{i,t}^{\mathrm{fair}}$, $\alpha_{i,t}$, $U_{i,t}$

Table 4
Constants and configuration parameters used in the AFGA algorithm.

Parameter	Value
ε	1×10^{-6}
λ	0.2
γ	0.5
PF	0.95
ULF_{max}	10%
V_{phase}	230
$\mathscr{C}_1$	7
$\mathscr{C}_2$	1.6

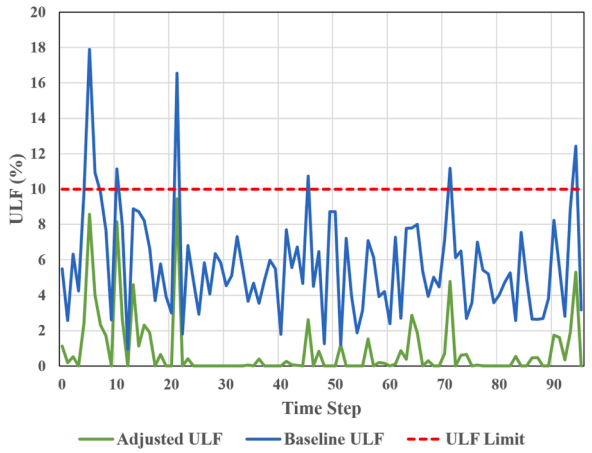

Fig. 7. Comparison of the baseline ULF (blue) and the adjusted ULF after demand reshaping (green) across all time steps. The red dashed line indicates the operational threshold of 10%.

AFGA procedure are distributed between the grid operator and participating consumers. The grid's total benefit amounted to €2911.49, computed using the net objective function defined in Eq. (15), which incorporates both the reward for ULF reduction (a positive contribution) and the cost of procuring flexibility (a negative contribution), as defined in Eq. (13) and Eq. (14), respectively. On the consumer side, the total accumulated benefit was €213.22, derived from the aggregated net utility across all users, as formulated in Eq. (12). This value encapsulates three key components: the reward for providing flexibility, the discomfort incurred due to load adjustments, and the fairness-aware penalty, as defined in Eq. (8), Eq. (9) and Eq. (10), respectively. The grid-to-consumers benefit ratio is therefore approximately 13.65, obtained by dividing the grid's total benefit (€2911.49) by the consumer's total benefit (€213.22). It should be noted that the consumer benefit corresponds to 20 consumers over a 24-hour period, which translates into an average daily benefit of about €10.66 per consumer under the simulation conditions considered here.

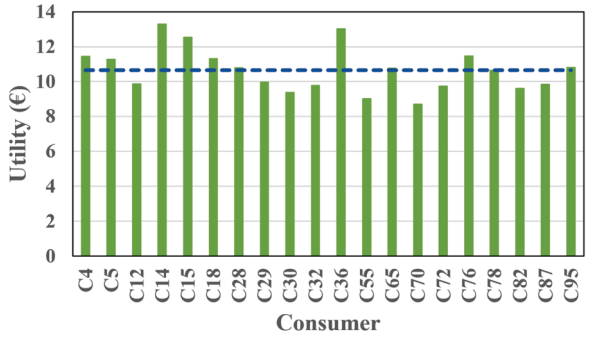

Fig. 8. Total accumulated utility (€) for each participating consumer over the simulation horizon. The blue dashed line represents the average utility across all consumers.

4.3. Fairness among consumers

This subsection evaluates the fairness of benefit allocation across the participating consumers, based on the accumulated utility derived from the optimization procedure. Fairness is a key objective embedded in the AFGA model through the fair allocation mechanism (Eq. (21)) and the penalty structure for over-contribution (Eq. (10)), with dynamic adjustments governed by Eq. (23). Fig. 8 shows the total accumulated utility, expressed in euros (€), obtained by each participating consumer over the entire simulation horizon. This figure provides an overview of how the economic benefits resulting from the proposed AFGA framework are distributed among consumers.

To further assess distributional equity, Fig. 9 presents the Lorenz curve, which depicts the cumulative share of total utility against the cumulative share of consumers. The closer the curve lies to the 45-degree line of perfect equality, the more equitable the utility allocation. Based on this curve, the corresponding Gini index is calculated as 0.065, indicating a very low level of inequality in the distribution of utility among consumers.

4.4. Adaptive control effectiveness for consumer C14 and C55

This subsection explores the dynamic behavior of the AFGA procedure at the individual level by analyzing two representative consumers: C14 and C55. These cases illustrate the model's adaptability in adjusting flexibility allocations, enforcing fairness, and tracking deviation penalties over time. Fig. 10 and Fig. 11 illustrate the time evolution of four key variables for consumers C14 and C55, respectively. The flexibility adjustment $x_{i,t}$ represents the actual demand modification implemented by each consumer. The fair allocation $x_{i,t}^{fair}$ denotes the proportional share of total phase-level flexibility expected from the consumer, as defined in Eq. (21). The available flexibility $f_{i,t}$ indicates the feasible adjustment range defined by each consumer's physical capabilities. Finally, the fairness penalty weight $\alpha_{i,t}$, is a dynamically updated coefficient that regulates the strength of penalization, as described in Eq. (23). For both consumers, the results show that the AFGA maintains flexibility adjustments within feasible limits while progressively aligning actual contributions with their expected fair allocations.

Fig. 12 and Fig. 13 depict the deviation between actual and fair flexibility contributions $\left(x_{i,t} - x_{i,t}^{fair}\right)$, alongside the corresponding evolution of the fairness penalty weight $\alpha_{i,t}$, for C14 and C55, respectively. These figures illustrate the feedback mechanism embedded in the AFGA framework: sustained over-contribution leads to a gradual increase in $\alpha_{i,t}$, which in turn raises the modeled cost associated with unfair participation in the objective function, as defined in Eq. (10). It is important to note that this penalty does not represent a direct cost imposed on the consumer; rather, it acts as an internal optimization mechanism that guides the allocation process. This adaptive loop discourages repeated imbalance and lies at the core of the fairness-enforcing logic of the AFGA framework. To quantify this dynamic, the Pearson correlation coefficient between the absolute deviation $|x_{i,t} - x_{i,t}^{fair}|$ and the corresponding fairness penalty $\alpha_{i,t}$ was computed. For consumer C14, the correlation is $r = 0.15$ ($p = 0.16$), whereas for consumer C55, it is stronger at $r = 0.27$ ($p = 0.0072$). These positive correlation values confirm that the fairness penalty responds consistently to the degree of over-contribution.

4.5. Computational performance

This subsection presents the computational efficiency of the proposed AFGA algorithm, with a focus on runtime and memory usage. These indicators are critical for evaluating the feasibility of deploying the model in near real-time residential grid environments. The simulation considers 100 residential users, of which only 20 participated in the RDR program. This low participation rate increases the optimization challenge, as the algorithm must still satisfy objectives such as fairness and ULF reduction while working with limited flexibility. The temporal horizon spans one full day, with a 15-minute resolution, resulting in 96 time slots per user and a total of 3,600

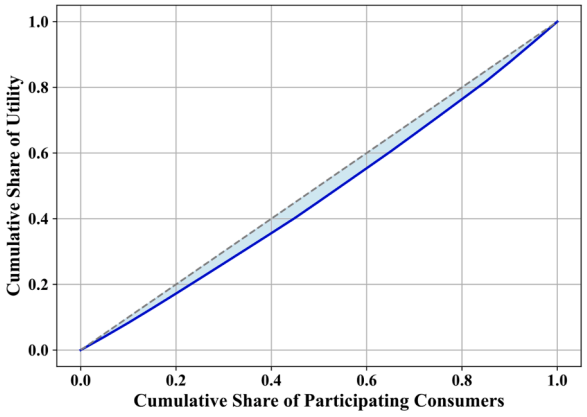

Fig. 9. Lorenz curve illustrating the cumulative distribution of total utility among participating consumers. The shaded area between the curve and the line of perfect equality indicates the degree of utility inequality.

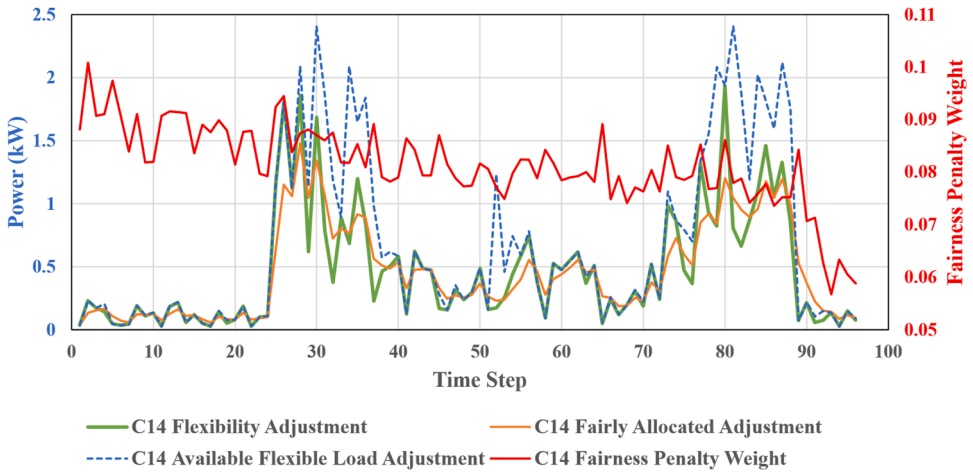

Fig. 10. Evolution of consumer C14's flexibility adjustment, fair allocation, available flexibility, and fairness penalty weight over the simulation horizon.

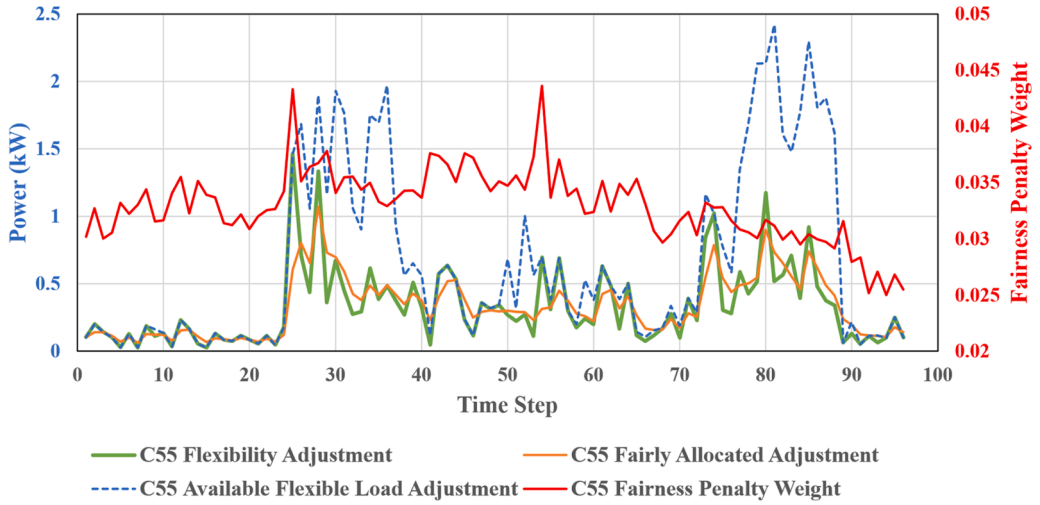

Fig. 11. Evolution of consumer C55's flexibility adjustment, fair allocation, available flexibility, and fairness penalty weight over the simulation horizon.

data points (i.e., 100 users × 96-time intervals). Table 5 summarizes the total computation time and peak memory usage required to optimize load schedules across all participants over the entire planning horizon.

4.6. Sensitive analysis of the fairness adaptation rate

The AFGA algorithm relies on a set of parameters and constants governing numerical stability, fairness adaptation, and grid-consumer trade-offs, as shown in Table 4. Among these, the fairness adaptation rate λ determines how rapidly historical deviations from the expected fair contribution influence the fairness penalty weight $\alpha_{i,t}$. While from Section 4.1 to Section 4.5 the effectiveness of AFGA algorithm is demonstrated using a value of $\lambda = 0.2$, this subsection evaluates the robustness of the algorithm to variations in this parameter.

To this end, a sensitive analysis is conducted by repeating the full-day simulation under three values of the fairness adaptation rate: $\lambda \in \{0.2, 0.5, 0.8\}$. The remaining parameters are fixed in order to isolate the impact of the fairness adaptation dynamics. The selected values for λ span a representative range from mild to aggressive fairness adaptation. This allows the evaluation of the key metrics shown in Table 6 for multiple scenarios. The key metrics are computed over the entire planning horizon for each value of λ. All simulations use identical demand and flexibility profiles, phase assignments, and random seeds to ensure comparability across scenarios.

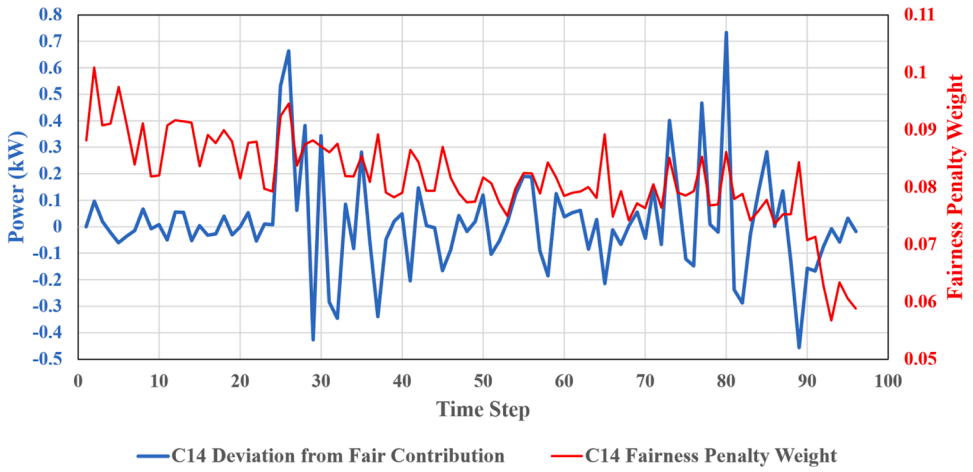

Fig. 12. Time evolution of the deviation between consumer C14's actual and fair contribution and the corresponding fairness penalty weight.

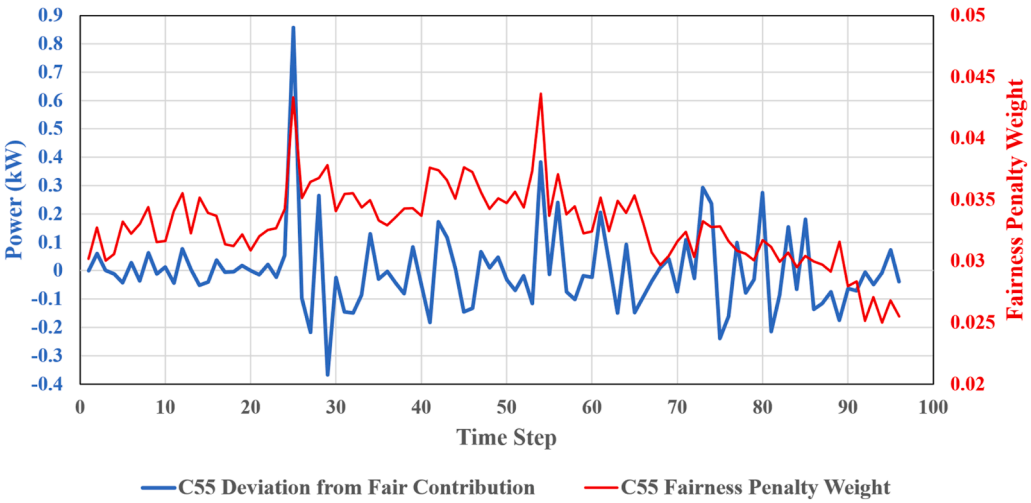

Fig. 13. Time evolution of the deviation between consumer C55's actual and fair contribution and the corresponding fairness penalty weight.

Table 5
Computational performance metrics for AFGA execution.

Metric	Value
Total optimization time	102.07 s
Peak memory usage	0.24 MB

Table 6
Impact of the fairness adaptation rate on ULF, fairness indicators and computational cost.

	$\lambda = 0.2$	$\lambda = 0.5$	$\lambda = 0.8$
Average value of adjusted ULF	0.89	0.89	0.89
Grid-to-consumers benefit ratio	13.65	13.65	13.64
Gini index	0.065	0.065	0.065
(r, p) for C14	(0.15, 0.16)	(0.094, 0.36)	(0.056, 0.59)
(r, p) for C55	(0.27, 0.0072)	(0.26, 0.010)	(0.27, 0.0075)
Total optimization time (s)	102.07	109.47	110.60
Peak memory usage (MB)	0.24	0.25	0.25

5. Discussion

5.1. Impact on ULF reduction

The AFGA procedure demonstrates a consistent and robust mitigation of ULF across the entire simulation horizon. As shown in Fig. 7, the adjusted ULF remains not only below the operational limit but persistently under the baseline. Compared with benchmark models in the literature, the proposed AFGA exhibits clear advantages.

For instance, the strategy proposed by [32] adopts a correlated equilibrium-based game-theoretic framework to coordinate appliance scheduling among residential users. While this achieves to a peak-to-average ratio (PAR) reduction of approximately 31.4%, the model does not address phase-level unbalance and does not incorporate explicit fairness metrics or voltage-related constraints in its optimization formulation. Although procedural fairness is considered in the form of rotating user priority during scheduling, no quantitative fairness objectives (e.g., utility equity) are embedded in the optimization problem.

Similarly, the decentralized RDR scheme proposed by [33] is focused primarily on energy volume balancing and user engagement. It does not incorporate grid-side constraints, such as voltage profiles or phase-level load unbalance, into the optimization process. As a result, while the method enhances scalability and appliance-level participation, it does not directly contribute to ULF mitigation or phase-aware load balancing at the distribution level.

In contrast, the AFGA procedure explicitly integrates phase-level ULF constraints together with fairness-aware control. While the results reported in [21] achieve lower voltage unbalance magnitudes (typically below 0.5% for three-phase buses) through specialized hardware, the AFGA algorithm demonstrates comparable capability to maintain unbalance within regulatory limits solely through smart load management.

5.2. Economic benefit sharing

The benefit-sharing structure of the proposed AFGA model resulted in a grid-to-consumer benefit ratio of approximately 13.65:1. While this may initially appear imbalanced, it is consistent with patterns observed in centralized, utility-driven RDR programs, where the grid acts as the primary stakeholder and system coordinator. Empirical evidence supports this dynamic; for instance, in a 20% participation scenario of a direct load control (DLC) program in Alberta, Canada [34], the grid-to-consumer benefit ratio was approximately 13.66:1, with operational cost savings of $40.3 million compared to $2.95 million in household savings.

5.3. Fairness among consumers

While there is noticeable variation among individual consumers, as shown in Fig. 8, the distribution of benefits remains closely centered around the group average (indicated by the blue dashed line), suggesting a moderate and well-regulated spread. Fairness among consumers is supported by both quantitative and visual evidence. Quantitatively, the Gini index is used to assess distributional equity, and its value of 0.065 indicates a very low level of inequality, reflecting a highly fair allocation. Visually, the Lorenz Curve presented in Fig. 9 corroborates this result, lying close to the line of perfect equality. The obtained Gini index is also consistent with values reported in the literature. For example, in the study by [29], which applied the Gini index to assess fairness in power system reliability across Norwegian regions and consumer groups, values ranged from 0.24 to 0.49 over a 12-year period– representing moderate to high inequality. This comparison underscores the strong fairness performance of the proposed AFGA procedure, with a Gini index value of 0.065.

5.4. Adaptive control in individual cases

Beyond aggregate fairness metrics, the AFGA model demonstrates a notable capability for user-specific adaptive control, enabling the system to respond dynamically to individual consumer behavior. This capability is illustrated through the case studies of consumers C14 and C55, as shown in Fig. 10, Fig. 11, Fig. 12, and Fig. 13. Although both consumers remain within their predefined flexibility bounds throughout the simulation horizon, they exhibit distinct fairness trajectories shaped by their unique response patterns and system interactions.

A key metric of this adaptivity is the Pearson correlation between the magnitude of deviation $|x_{i,t} - x_{i,t}^{fair}|$ and the associated penalty weight $\alpha_{i,t}$. For C14, the correlation was weak and positive but not statistically significant ($r = 0.15, p = 0.16$). In contrast, C55 showed a small-to-moderate positive correlation that was statistically significant ($r = 0.27, p = 0.0072$). This contrast highlights that the AFGA procedure does not apply a static, uniform penalization approach but instead dynamically learns and adapts its response for each user, thereby enhancing both individual fairness and system responsiveness.

Unlike the framework proposed in [19]–which schedules loads using mixed-integer linear programming (MILP) based on consumption and production forecasts, and employs reinforcement learning (RL) to provide robustness against uncertainties and deviations from these initial forecasts, the AFGA algorithm demonstrates that, even in a stochastic context, flexibility activation can be coordinated in a fair and grid-supported manner.

5.5. Computational performance

The practical deployment of demand response events in residential distribution systems depends not only on the quality of the optimization model but also on its computational feasibility. In this regard, the AFGA algorithm completes a full-day simulation in 102 seconds with a peak memory usage of 0.24 MB, as reported in Table 5. This performance is particularly notable given the simulation's scale and complexity. Although the total system comprises 100 households, only 20 users were enrolled in the RDR program, representing a low participation rate of 20%. This setup presents a near-critical optimization challenge, as the AFGA algorithm must satisfy demanding objectives, including fairness enforcement and ULF reduction, while operating with limited available flexibility. Despite this constraint, the algorithm successfully converged within the execution window. Importantly, the scenario studied in this research represents a typical residential area supplied by a single low-voltage distribution feeder, as commonly found in many urban zones. The algorithm and simulation are thus intentionally scaled to match this realistic grid configuration. For this reason, further scaling the number of participants—solely to test algorithmic limits—is not central to the scope of this work.

5.6. Sensitivity to the fairness adaptation rate

The sensitivity analysis in Section 4.6 evaluates the robustness of the proposed AFGA algorithm against variations in the fairness adaptation rate λ, which dictates how rapidly historical deviations from fair contributions influence the fairness penalty weight. The results in Table 6 show that the algorithm's outputs remain stable across a wide range of λ values. Notably, the average ULF remains constant across all tested cases, demonstrating that grid-level performance and phase unbalance reduction are insensitive to the speed of fairness adaptation. Similarly, the grid-to-consumers benefit ratio and the Gini index exhibit negligible variation, indicating that economic efficiency and equity are preserved even under aggressive adaptation dynamics. While Pearson correlation coefficients between fairness deviations and penalty weights show moderate variation–reflecting diverse individual flexibility patterns–these fluctuations do not affect aggregate fairness or grid performance. This suggests the adaptive penalty mechanism remains effective without inducing instability. From a computational perspective, increasing λ leads to only a modest increase in total optimization time and memory usage.

5.7. Summary of results and literature comparison

Table 7 summarizes the primary outcomes of the proposed AFGA algorithm across five key dimensions: ULF reduction, economic benefit sharing, fairness, adaptivity, and computational performance. Compared to related studies, AFGA distinguishes itself by explicitly integrating fairness-aware control with grid-side constraints, achieving a superior balance between technical robustness, equity, and operational feasibility. The simulation scenario assumes a high degree of heterogeneity in flexibility: only 20% of residential users participate in the demand response program, while the remainder are fully inflexible. This configuration represents an extreme yet realistic scenario typical of early program adoption. As demonstrated in Sections 5.1 and 5.3, the proposed AFGA algorithm maintains effective phase unbalance mitigation and equitable benefit allocation even under these highly heterogeneous conditions.

6. Conclusions

This article introduced the AFGA procedure, a novel approach designed to reduce phase unbalance in low-voltage residential distribution networks while ensuring equitable consumer participation during RDR events. The proposed method explicitly considers phase unbalance reduction as a primary grid-level objective and integrates fairness constraints directly into the flexibility allocation process.

Table 7
Comparative summary of AFGA algorithm results and related works. An '–' indicates that a feature is not addressed or reported in the corresponding reference.

Aspect	This work	[32]	[33]	[21]	[34]	[29]	[19]
ULF/phase-level unbalance	ULF within regulatory limits	PAR < 31.4%	–	ULF < 0.5%	–	–	–
Fairness/equity	Gini index = 0.065	Rotating priority	User engagement emphasized	–	–	Gini index = 0.24-0.49	–
Economic benefit sharing	Grid-to-consumer ratio ≈ 13.65:1	–	–	–	Grid-to-consumer ratio ≈ 13.66:1	–	–
Adaptivity (user-specific response)	(r, p) for C14 and C55	–	–	–	–	–	RL-based adaptivity to uncertainty
Computational performance	Full-day simulation in 102 s; peak memory 0.24 MB	–	–	Hardware solution	–	–	MILP + RL

The main contributions of this work are threefold. First, it establishes phase unbalance reduction as a primary grid-level objective within the optimization formulation, i.e., in both the objective function and the constraints. Second, the allocation procedure is applied to consumers whose flexibility profiles are modeled by accounting for time-dependent and appliance-level behavior, rather than relying on fixed flexibility agreements. Third, the proposed fairness control mechanism is adaptive and grounded in a Nash bargaining framework, penalizing persistent over-contribution to prevent exploitation and promote equitable participation over time. This integration of physical grid constraints with social equity principles represents an important advance in fairness-aware demand response schemes.

Simulation results demonstrate the effectiveness of the AFGA procedure across multiple dimensions. Phase unbalance, measured by the ULF, was consistently reduced below baseline values and maintained within operational thresholds, even with a low participation rate of 20%. Fairness was quantitatively validated by a Gini index of 0.065, indicating a highly equitable distribution of utility among participating consumers. In addition, the adaptive control mechanism was confirmed through positive correlations between deviations from fair contributions and the corresponding penalty weights for representative consumers, highlighting the responsiveness and stability of the fairness enforcement strategy.

Beyond its theoretical contributions, the proposed AFGA framework aligns closely with emerging RDR programs currently being adopted in practice. For example, recent initiatives in Australia enable residential air conditioners to provide flexible demand support to the electricity grid through voluntary participation, thereby improving system reliability and operational efficiency. In this context, the AFGA algorithm offers a fairness-aware mechanism for coordinating residential TCL-based flexibility. By explicitly accounting for user heterogeneity, historical participation, and grid-level constraints, the proposed approach addresses key practical challenges such as consumer acceptance, equitable participation, and scalability. As a result, AFGA can serve as an effective decision-support tool for aggregators or distribution system operators implementing RDR programs.

Future research will extend the AFGA framework toward more comprehensive smart grid applications. This includes incorporating distributed generation sources such as rooftop photovoltaics, integrating energy storage systems such as electric vehicles, utilizing real-time appliance-level data, and exploring decentralized and peer-to-peer coordination frameworks, longer-term participation dynamics, and incentive adaptation. Finally, an important future direction will be the application of the AFGA algorithm in a real low-voltage distribution network within a practical setting, such as an urban neighborhood, to assess its performance under real-world operating conditions. These extensions will build upon the current AFGA algorithm, enhancing its relevance and applicability in future smart grid environments.

Author Contribution All authors contributed to the study conception and design. Material preparation, data collection and analysis were performed by all authors. The first draft of the manuscript was written by Gabriel Gómez-Ruiz and all authors commented on previous versions of the manuscript. All authors read and approved the final manuscript.

Declaration of competing interest

The authors have no competing interests to declare that are relevant to the content of this article.

Declaration of competing interest

The authors declare that they have no known competing financial interests or personal relationships that could have appeared to influence the work reported in this paper.

Acknowledgements

This article is part of the project “Integral control system to optimize the microgrids energy demand”, grant number PID2020-117828RB-I00, funded by the Spanish Ministry of Science, Innovation and Universities. The author Gabriel Gómez-Ruiz is enjoying an FPU grant, number FPU21/00468, funded by the Spanish Ministry of Science, Innovation and Universities for the training of university teaching staff during his PhD period. Funding for open access charge: Universidad de Huelva / CBUA.

Data availability

Data will be made available on request.

References

[1] Ma K, Fang L, Kong W. Review of distribution network phase unbalance: scale, causes, consequences, solutions, and future research directions. CSEE J Power Energy Syst Sept. 2020;6(3):479–88. https://doi.org/10.17775/CSEEJPES.2019.03280.

[2] Sánchez-Herrera R, Clavijo-Camacho J, Gómez-Ruiz G, Vázquez JR. Identification of both distortion and imbalance sources in electrical installations: a comparative assessment. Energy Jan. 2024;17(11). https://doi.org/10.3390/en17112536. Art. no. 11.

[3] Arghavani H, Peyravi M. Unbalanced current-based tariff. CIRED Oct. 2017;2017(1):883–7. https://doi.org/10.1049/oap-cired.2017.0129.

[4] “Motors and generators, ” NEMA. Accessed: Aug. 15, 2025. [Online]. Available: https://www.nema.org/standards/view/motors-and-generators.

[5] Herrera RS, Vázquez JR. Identification of unbalanced loads in electric power systems. Int Trans Electr Energy Syst 2014;24(9):1232–43. https://doi.org/10.1002/etep.1772.

[6] Martin AD, Herrera RS, Vazquez JR, Crolla P, Burt GM. Unbalance and harmonic distortion assessment in an experimental distribution network. Electr Power Syst Res Oct. 2015;127:271–9. https://doi.org/10.1016/j.epsr.2015.06.005.

[7] Okeke D, Gryazina E, Ibanez FM, Albaseer A, Abdallah M. Coordinated control of distributed thermostatically controlled load for frequency regulation and impact on voltage profile of a microgrid. In: 2024 13th International Conference on Renewable Energy Research and Applications (ICRERA); Nov. 2024. p. 212–6. https://doi.org/10.1109/ICRERA62673.2024.10815540.

[8] Gyamfi S, Krumdieck S. Price, environment and security: exploring multi-modal motivation in voluntary residential peak demand response. Energy Policy May 2011;39(5):2993–3004. https://doi.org/10.1016/j.enpol.2011.03.012.
[9] Wang J, Huang Q. Minimization of network losses with financial incentives in voluntary demand response. IEEe Access 2018;6:16515–22. https://doi.org/10.1109/ACCESS.2018.2797272.
[10] Haider HT, See OH, Elmenreich W. A review of residential demand response of smart grid. Renew Sustain Energy Rev June 2016;59:166–78. https://doi.org/10.1016/j.rser.2016.01.016.
[11] Zheng W, Wu W, Zhang B, Lin C. Distributed optimal residential demand response considering operational constraints of unbalanced distribution networks. IET Gener Transm Distrib 2018;12(9):1970–9. https://doi.org/10.1049/iet-gtd.2017.1366.
[12] Kumar NM, et al. Distributed energy resources and the application of AI, IoT, and blockchain in smart grids. Energy Jan. 2020;13(21):5739. https://doi.org/10.3390/en13215739.
[13] Clavijo-Camacho J, Ruiz-Rodríguez FJ, Sánchez-Herrera R, Alamo AC. Advanced Distribution System optimization: utilizing flexible power buses and network reconfiguration. Appl Sci Jan. 2024;14(22). https://doi.org/10.3390/app142210635. Art. no. 22.
[14] Gomez-Ruiz G, Sanchez-Herrera R, Andujar JM, Rubio Sanchez JL. Simulation-based education tool for understanding thermostatically controlled loads. Sustainability Jan. 2024;16(3). https://doi.org/10.3390/su16030999. Art. no. 3.
[15] Residential Demand Response Program (RDRP),” Canada: Government of Canada. Accessed: June 30, 2025 [Online]. Available: https://natural-resources.canada.ca/funding-partnerships/residential-demand-response-program-rdrp.
[16] Soares J, et al. Review on fairness in local energy systems. Appl Energy Nov. 2024;374:123933. https://doi.org/10.1016/j.apenergy.2024.123933.
[17] Shao C, Feng C, Zhang X, Tang H, Liu J. Optimization method based on load forecasting for three-phase imbalance mitigation in low-voltage distribution network. In: 2022 IEEE 5th International Electrical and Energy Conference (CIEEC); May 2022. p. 1032–7. https://doi.org/10.1109/CIEEC54735.2022.9846003.
[18] Zhou L, et al. Multi-objective optimisation operation of thermostatically controllable appliances for voltage management in low-voltage distribution networks. IET Gener Transm Distrib Nov. 2019;13(21):4767–77. https://doi.org/10.1049/iet-gtd.2019.0814.
[19] Felicetti R, Ferracuti F, Iarlori S, Monteriù A. Peak shaving and self-consumption maximization in home energy management systems: a combined integer programming and reinforcement learning approach. Comput Electr Eng July 2024;117:109283. https://doi.org/10.1016/j.compeleceng.2024.109283.
[20] Nourizadeh H, Nazar MS. Optimal day-ahead scheduling and reconfiguration of active distribution systems considering energy hubs, residential demand response aggregators, and electric vehicle parking lot aggregators. Comput Electr Eng Apr. 2025;123:110227. https://doi.org/10.1016/j.compeleceng.2025.110227.
[21] Ayazi AM, Shakarami MR, Doostizadeh M, Namdari F, Nikzad MR. Short-term optimal operation of phase shifting soft open point with high accuracy loss model in unbalanced distribution networks. Comput Electr Eng Apr. 2025;123:110284. https://doi.org/10.1016/j.compeleceng.2025.110284.
[22] Ali L, Muyeen SM, Bizhani H, Ghosh A. Comparative study on game-theoretic optimum sizing and economical analysis of a networked microgrid. Energ (Basel) Jan. 2019;12(20):4004. https://doi.org/10.3390/en12204004.
[23] Tushar W, et al. A motivational game-theoretic approach for peer-to-peer energy trading in the smart grid. Appl Energy June 2019;243:10–20. https://doi.org/10.1016/j.apenergy.2019.03.111.
[24] Pal S, Thakur S, Kumar R, Panigrahi BK. A strategical game theoretic based demand response model for residential consumers in a fair environment. Int J Electr Power Energy Syst Apr. 2018;97:201–10. https://doi.org/10.1016/j.ijepes.2017.10.036.
[25] Baharlouei Z, Hashemi M, Narimani H, Mohsenian-Rad H. Achieving optimality and fairness in autonomous demand response: benchmarks and billing mechanisms. IEEe Trans Smart Grid June 2013;4(2):968–75. https://doi.org/10.1109/TSG.2012.2228241.
[26] Gerdroodbari YZ, Khorasany M, Razzaghi R. Dynamic *PQ* operating envelopes for prosumers in distribution networks. Appl Energy Nov. 2022;325:119757. https://doi.org/10.1016/j.apenergy.2022.119757.
[27] Premkumar M, Ravichandran S, Hourani AO, Alghamdi TAH. Optimizing residential flexibility for sustainable energy management in distribution networks. Energy Rep Dec. 2024;12:4696–716. https://doi.org/10.1016/j.egyr.2024.10.034.
[28] Dewangan CL, et al. An improved decentralized scheme for incentive-based demand response from residential customers. Energy Dec. 2023;284:128568. https://doi.org/10.1016/j.energy.2023.128568.
[29] Heylen E, Ovaere M, Proost S, Deconinck G, Van Hertem D. Fairness and inequality in power system reliability: summarizing indices. Electr Power Syst Res Mar. 2019;168:313–23. https://doi.org/10.1016/j.epsr.2018.11.011.
[30] Pearson’s correlation coefficient. Encyclopedia of public health. Dordrecht: Springer; 2008. p. 1090–1. https://doi.org/10.1007/978-1-4020-5614-7_2569.
[31] Terven J, Cordova-Esparza D-M, Romero-González J-A, Ramírez-Pedraza A, Chávez-Urbiola EA. A comprehensive survey of loss functions and metrics in deep learning. Artif Intell Rev Apr. 2025;58(7):195. https://doi.org/10.1007/s10462-025-11198-7.
[32] Pal S, Thakur S, Kumar R, Panigrahi BK. A strategical game theoretic based demand response model for residential consumers in a fair environment. Int J Electr Power Energy Syst Apr. 2018;97:201–10. https://doi.org/10.1016/j.ijepes.2017.10.036.
[33] Dewangan CL, et al. An improved decentralized scheme for incentive-based demand response from residential customers. Energy Dec. 2023;284:128568. https://doi.org/10.1016/j.energy.2023.128568.
[34] Miri M, McPherson M. Demand response programs: comparing price signals and direct load control. Energy Feb. 2024;288:129673. https://doi.org/10.1016/j.energy.2023.129673.